Resonant terahertz detection using graphene plasmons

Igor Gayduchenko, Maxim Moskotin, Ivan Tretyakov, Gregory N. Goltsman
Moscow State University of Education

Dmitry Svintsov, Denis Yagodkin, Sergey Zhukov, Georgy Fedorov
Moscow Institute of Physics and Technology

Denis A. Bandurin, Alessandro Principi, Irina V. Grigorieva, Marco Polini, Andre K. Geim
School of Physics, University of Manchester

Shuigang G. Xu, Takashi Taniguchi, Kenji Watanabe
National Institute for Materials Science, Japan

Outline

- 1. Introduction:
- - What is THz radiation?
- - THz Detectors. Why graphene based?

- 2. The main mechanisms of THz radiation detection by graphene-based FET devices.

- 3. THz detection using FETs based on double layer graphene incapsulated in hBN:
- - Broadband detection
- - Resonant detection
- - THz spectroscopy of plasmons in graphene

- 4. Conclusions

Motivation

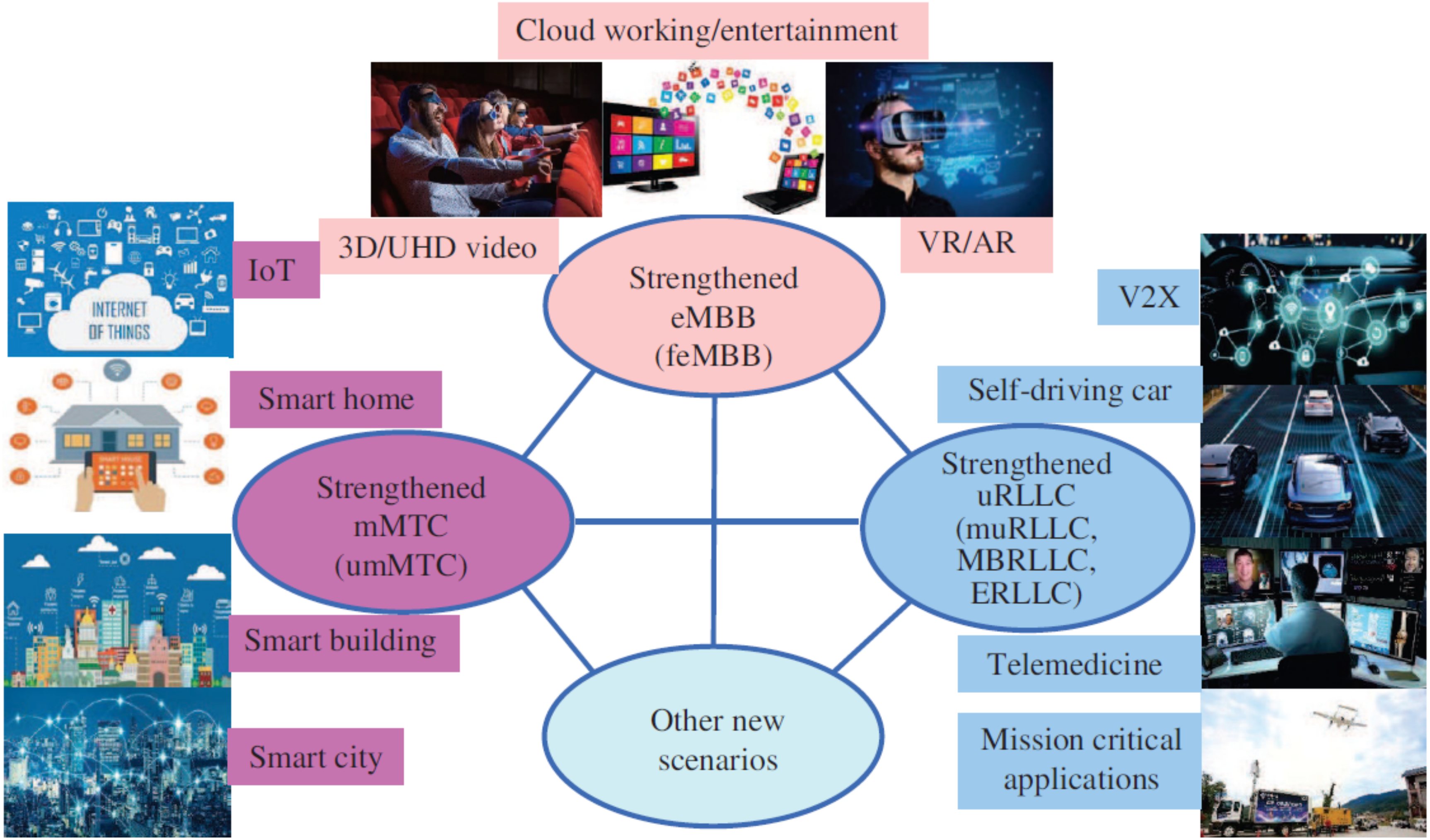

Problems:
- Modern THz radiation detectors either operate at low temperatures or are quite slow;
- It is necessary to develop new methods and approaches for detecting THz radiation.

MOTIVATION

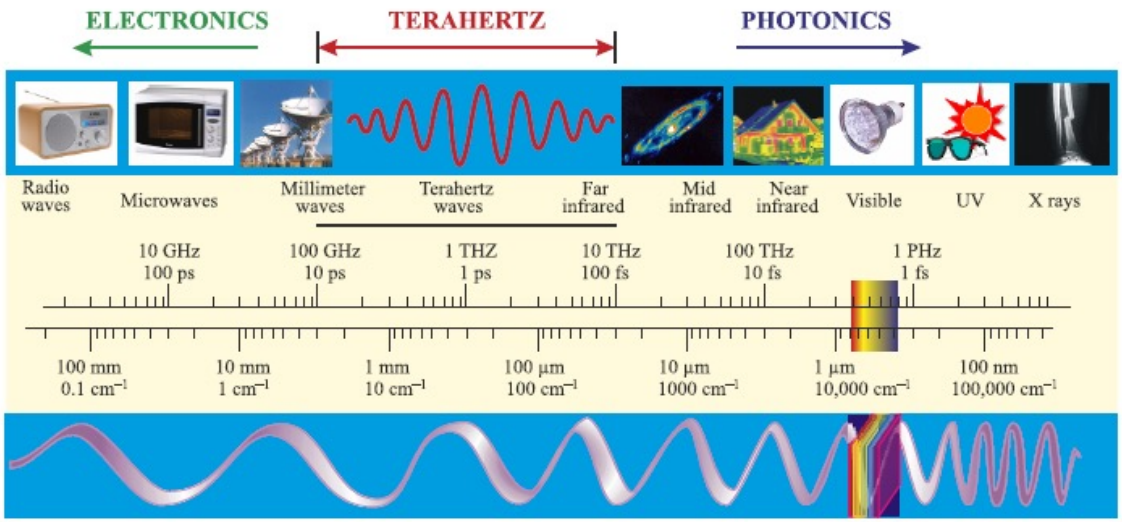

Detectors.

Why nanosturtures:

- Sensitive
- Fast
- Energy efficient
- Spectral sensitive

Detectors. Why graphene (CNT) based:

-Gapless graphene has strong interband absorption at all frequencies

- High room-temperature mobility

-Geometric control of the band structure

- Easy to fabricate

- The frequency of graphene plasma waves lies in the terahertz range

MOTIVATION

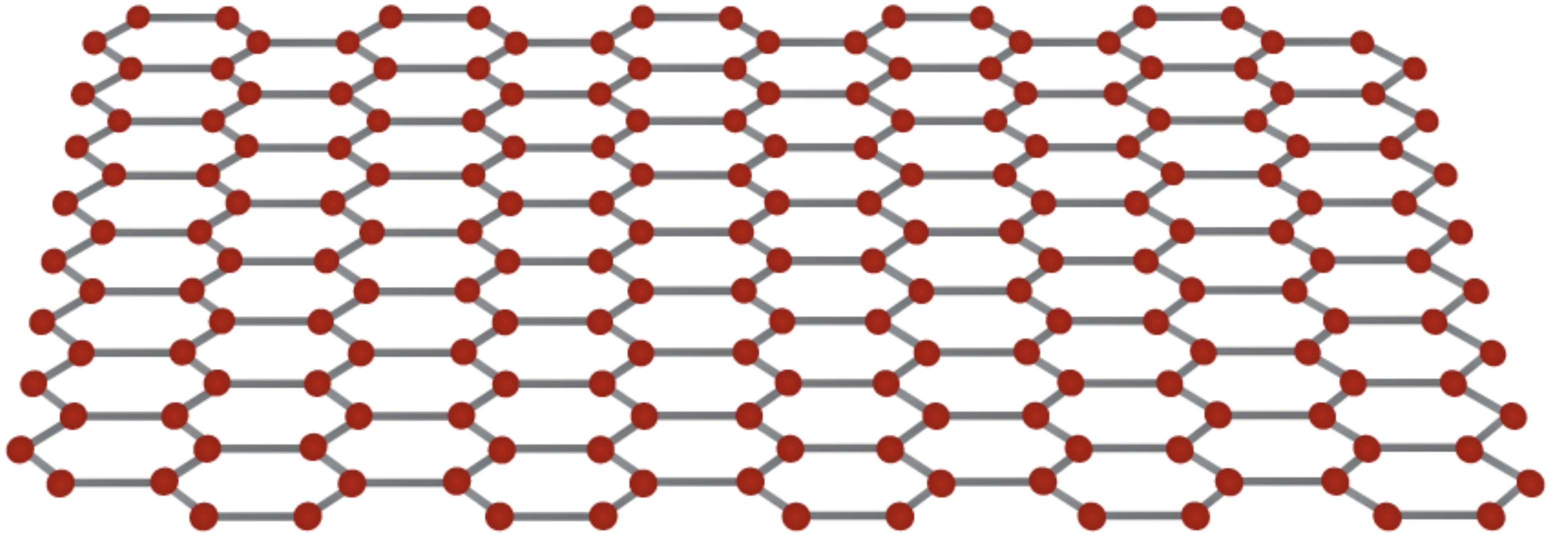

Detectors. Why graphene (CNT) based:

- -Gapless graphene has strong interband absorption at all frequencies
- - High room-temperature mobility
- -Geometric control of the band structure
- - Easy to fabricate
- - The frequency of graphene plasma waves lies in the terahertz range

MOTIVATION

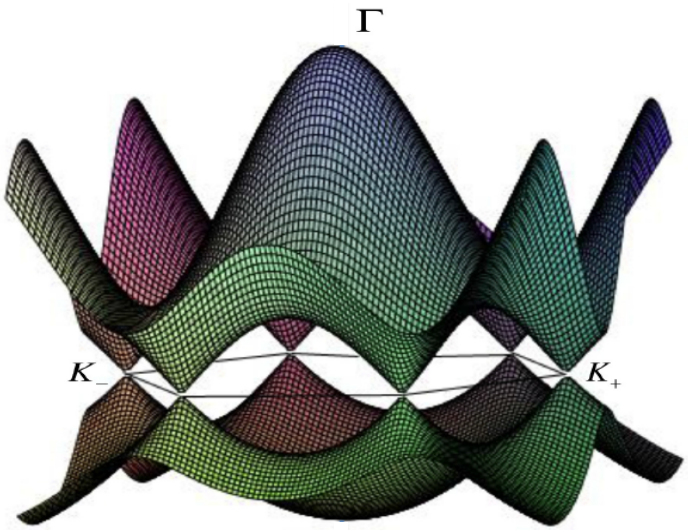

$$E(k) = E_0 + 2\gamma_1\left(\cos(\vec{k}\vec{a}_1) + \cos(\vec{k}\vec{a}_2) + \cos(\vec{k}(\vec{a}_1 - \vec{a}_2)\right)$$

$$\pm\gamma_0\sqrt{3 + 2\cos\vec{k}\vec{a}_1 + 2\cos\vec{k}\vec{a}_2 + 2\cos\vec{k}(\vec{a}_1 - \vec{a}_2)}$$

Detectors. Why graphene (CNT) based:

-Gapless graphene has strong interband absorption at all frequencies

- High room-temperature mobility

-Geometric control of the band structure

- Easy to fabricate

- The frequency of graphene plasma waves lies in the terahertz range

MOTIVATION

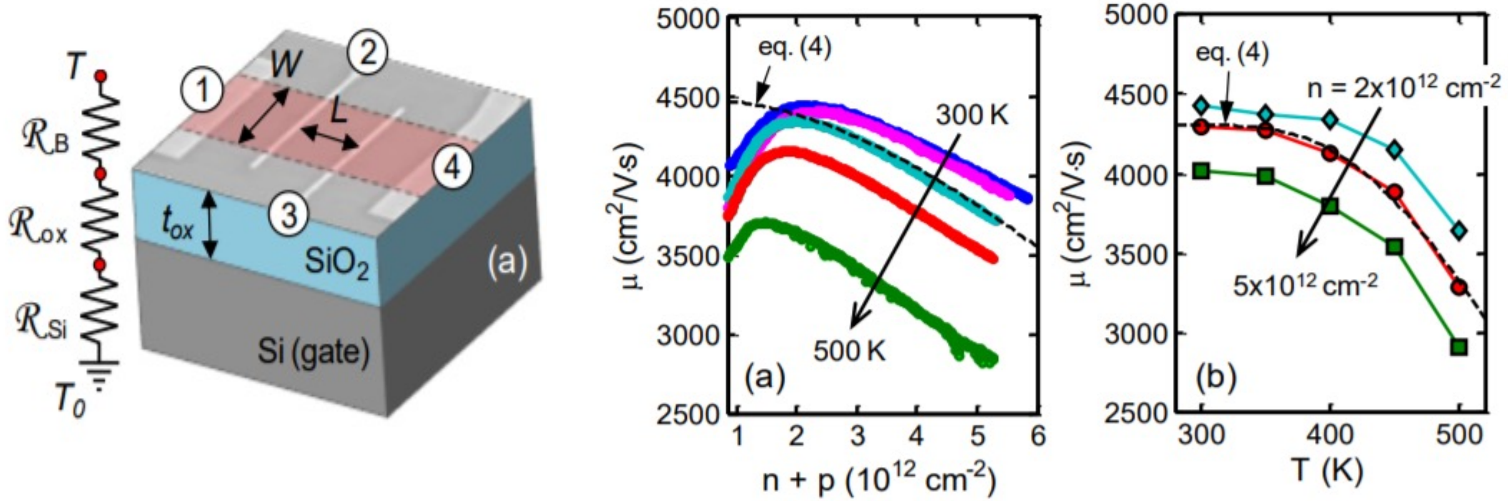

Detectors. Why graphene (CNT) based:

-Gapless graphene has strong interband absorption at all frequencies

- High room-temperature mobility

-Geometric control of the band structure

- Easy to fabricate

- The frequency of graphene plasma waves lies in the terahertz range

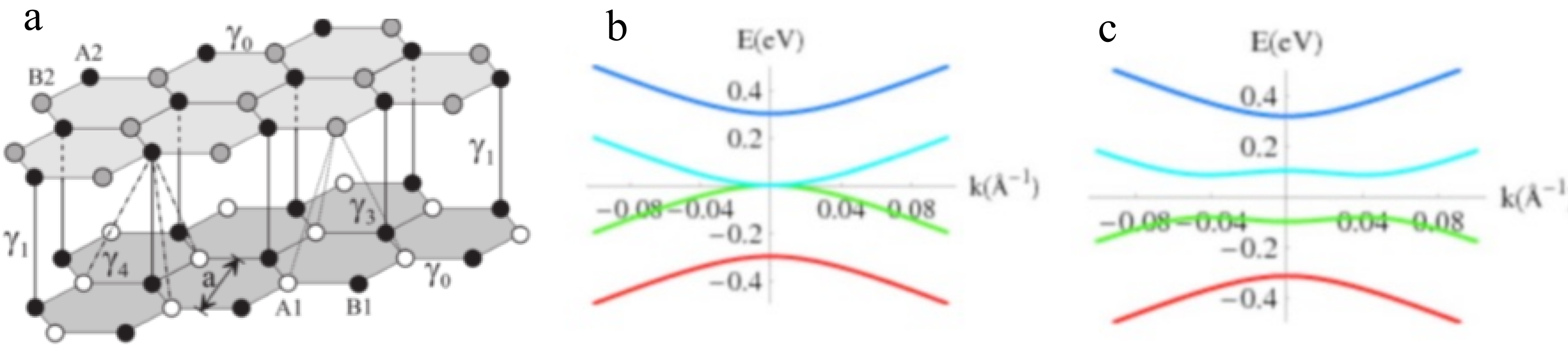

Detectors. Why graphene (CNT) based:

-Gapless graphene has strong interband absorption at all frequencies

- High room-temperature mobility

-Geometric and electrostatic control of the band structure

- Easy to fabricate

- The frequency of graphene plasma waves lies in the terahertz range

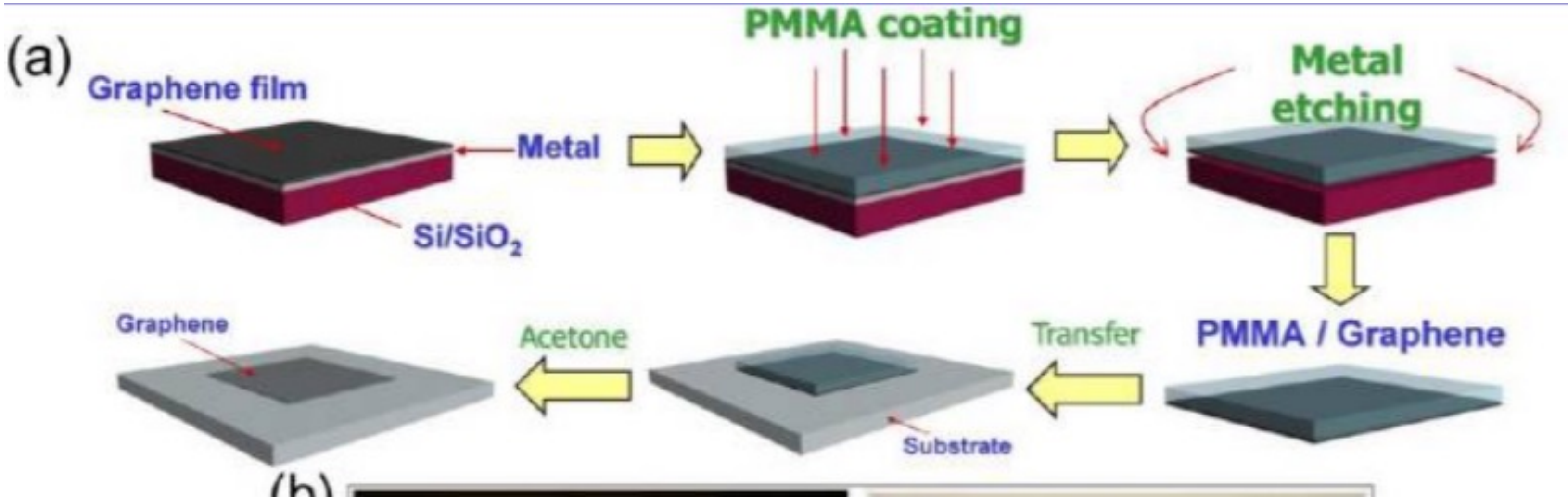

Detectors. Why graphene (CNT) based:

-Gapless graphene has strong interband absorption at all frequencies

- High room-temperature mobility

-Geometric control of the band structure

- Easy to fabricate

- The frequency of graphene plasma waves lies in the terahertz range

MOTIVATION

Plasmonics forms a major part of the fascinating field of *nanophotonics*, which explores how electromagnetic fields can be confined over dimensions on the order of or smaller than the wavelength.

Plasmonics: Fundamentals and Applications
Authors: Maier, Stefan Alexander
Springer, 2007

Detectors. Why graphene (CNT) based:

- **Gapless graphene has strong interband absorption at all frequencies**
- **High room-temperature mobility**
- **Geometric control of the band structure**
- **Easy to fabricate**
- **The frequency of graphene plasma waves lies in the terahertz range**

What do we mean by graphene THz detector

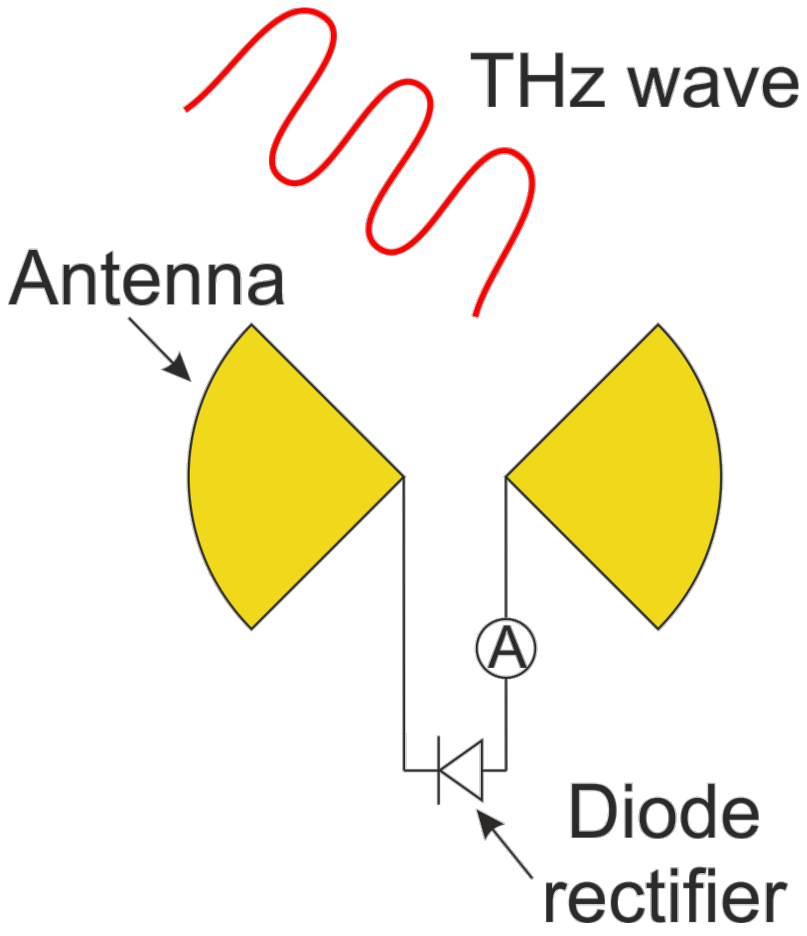

$$\left\langle I\left(\delta V\cos\omega t\right)\right\rangle_T \approx$$

$$\frac{dI}{dV}\delta V\left\langle\cos\omega t\right\rangle_T + \frac{1}{2}\frac{d^2I}{dV^2}\delta V^2\left\langle\cos^2\omega t\right\rangle_T$$

$$= \frac{1}{4}\frac{d^2I}{dV^2}\delta V^2$$

Study of detection mechanisms is the study of nonlinearities

The main mechanisms of THz radiation detection by graphene-based FET devices

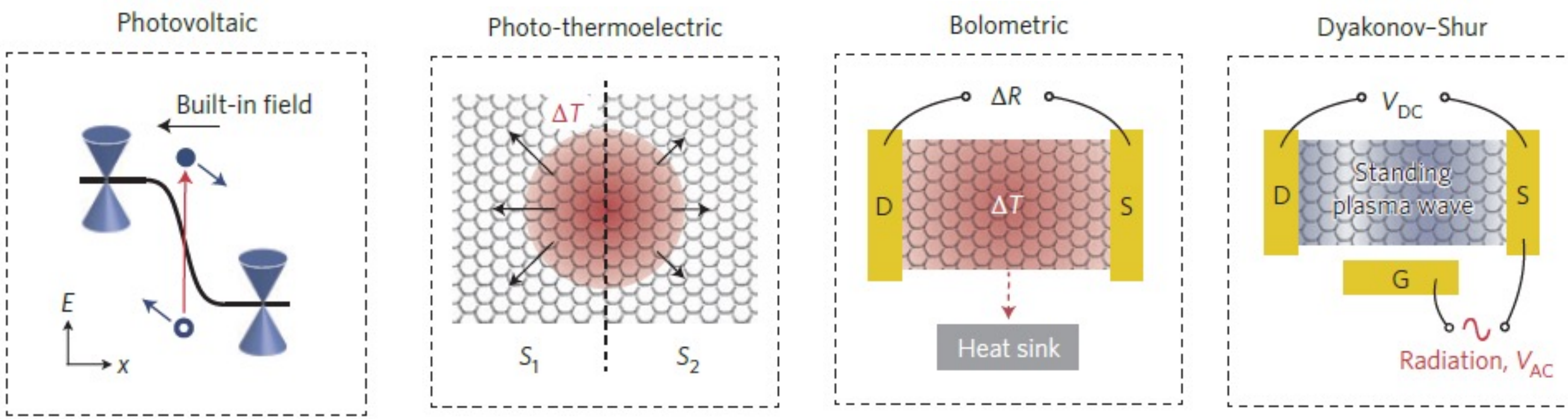

Current due to built-in field at the junction OR rectification due to diode nonlinearity

Voltage due to temperature gradients in nonuniformly doped channel

Resistance change due to overall device heating

Formation of standing plasma waves in the device channel

Figure from: F.H.L. Koppens, T. Mueller, P. Avouris, A.C. Ferrari, M.S. Vitiello, M. Polini, "Photodetectors based on graphene, other two-dimensional materials and hybrid systems" Nature nanotechnology, 9, 780-793 (2014)

Photo-thermoelectric effect in graphene

In case of a **photothermoelectric effect** an non-uniform doping of the channel and non-uniform heating of the channel results in onset of a DC voltage proportional to increase of the electron temperature

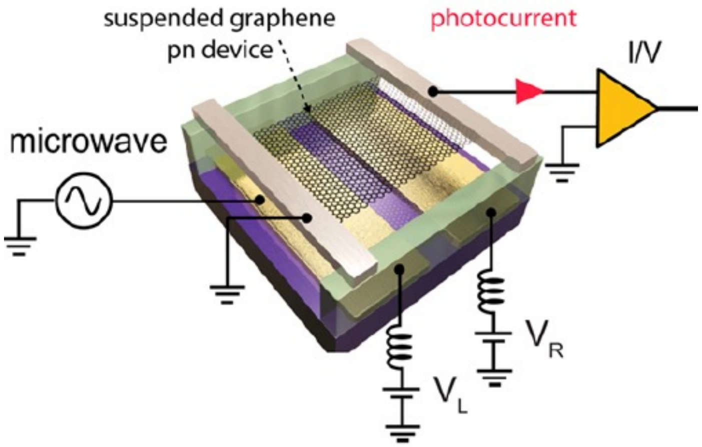

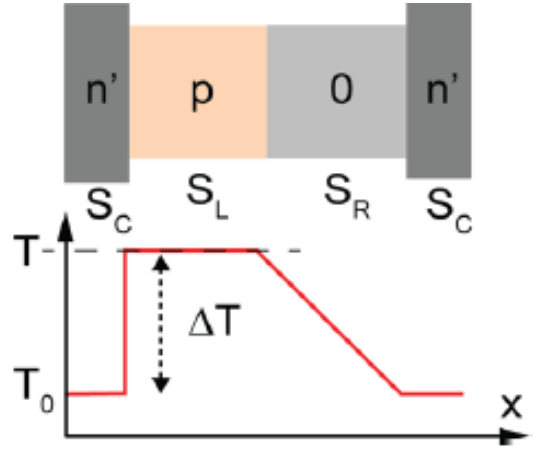

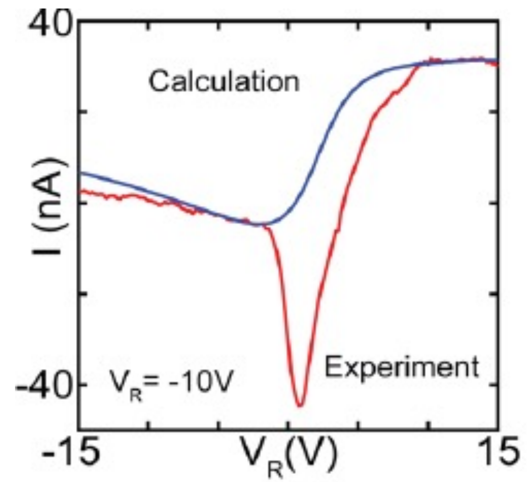

Graphene advantages for hot-electron photothermoelectric detection:

○-Gapless graphene has strong interband absorption at all frequencies.

○-The electronic heat capacity of single-layer graphene is much lower than in bulk materials, resulting in a larger change in temperature for the same absorbed energy

○- The photothermoelectric effect has a picosecond response time, set by the electron– phonon relaxation rate

Photo-thermoelectric effect

$$U_{PTE} = -\int S dT \approx S(T_S - T_D)$$

$$S \approx -\frac{\pi^2 k_B^2 T}{3e}\frac{1}{\sigma}\frac{d\sigma}{dE_F}$$

Nano Lett. ***16***, *6988 (2016)*

Photo-thermoelectric effect in graphene

Graphene photothermoelectric detector. Principle of operation

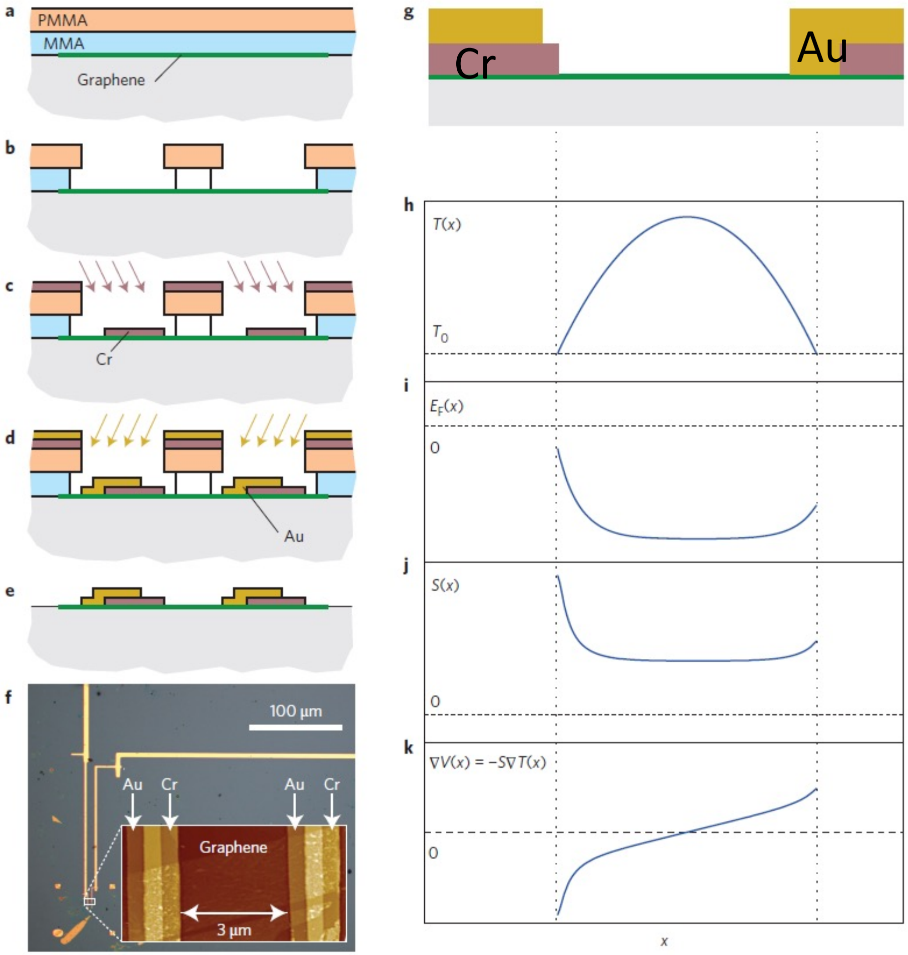

Graphene photothermoelectric detector device fabrication and principle of operation. (a-e) Lithographic sequence used to produce the graphene terahertz detector.(f) Optical micrograph showing electrical contacts and (inset) atomic force micrograph showing bimetallic contacts connected to an exfoliated graphene layer. (g-k) Schematic of the principle components during device operation. (g) Cross-sectional view of the device. (h-j) Profiles across the device of (h) electron temperature T(x), (i) Fermi level EF(x), (j) Seebeck coefficient S(x) and (k) potential gradient.

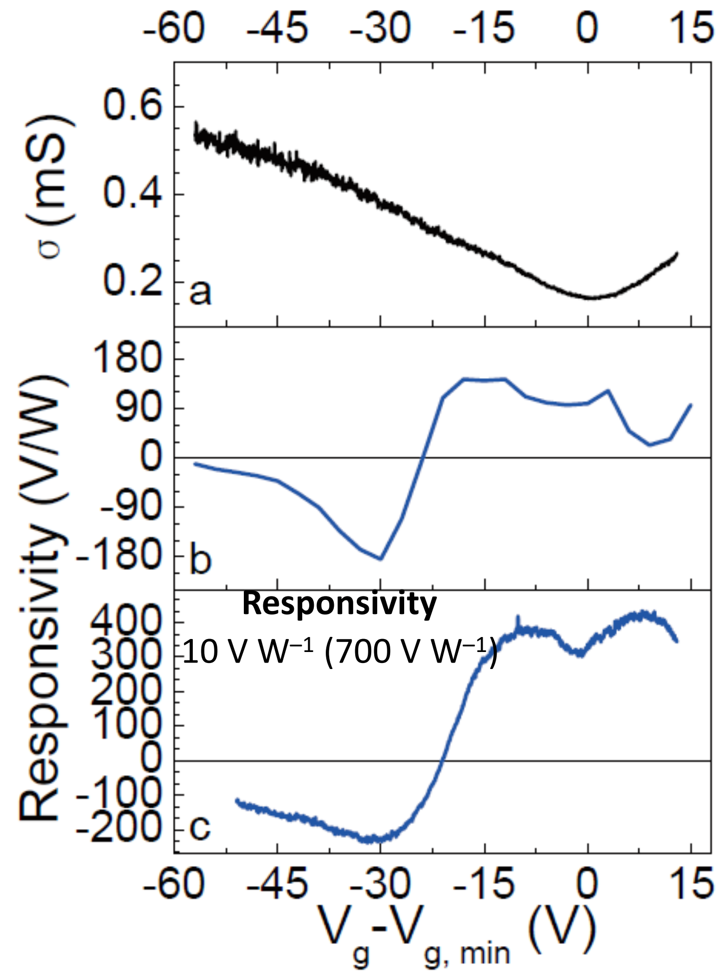

Broadband thermoelectric responsivity of graphene photothermoelectric detector. (a,d) Electrical conductance, (b,e) responsivity to Joule heating, and (c,f) responsivity to radiation as a function of gate voltage for the device shown in Fig. 1f at room temperature and in ambient environment.

Nature Nanotechnology* **9, 814–819 (2014)

Детектирование ТГц излучения за счет возбуждение плазмонов

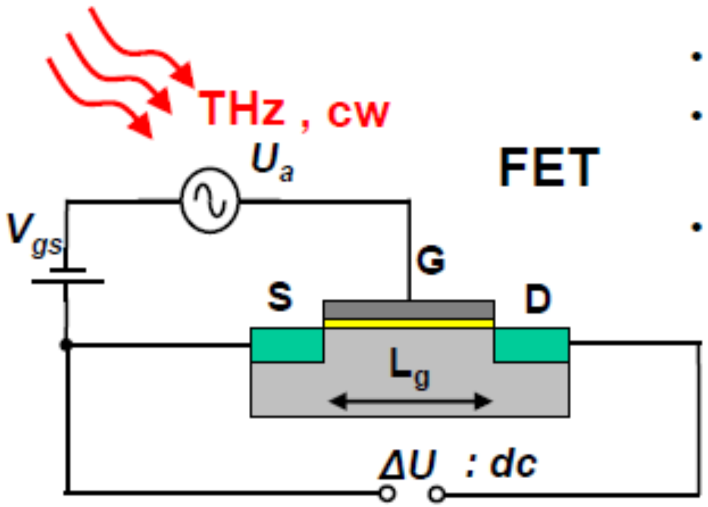

$$n_s = CU/e$$

$$\frac{\partial v}{\partial t} + v\frac{\partial v}{\partial x} + \frac{e}{m}\frac{\partial U}{\partial x} + \frac{v}{\tau} = 0$$

$$\frac{\partial U}{\partial t} + \frac{\partial (Uv)}{\partial x} = 0.$$

$$U(0,t) = U_o + U_a \cos \omega t \quad \text{for} \quad x = 0$$

$$j(L,t) = 0 \quad \text{for} \quad x = L$$

Resonant Detector *ωτ >> 1*

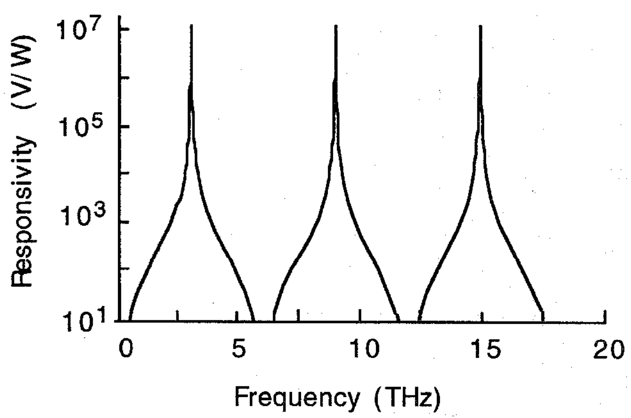

Broadband Detector ωτ <<1

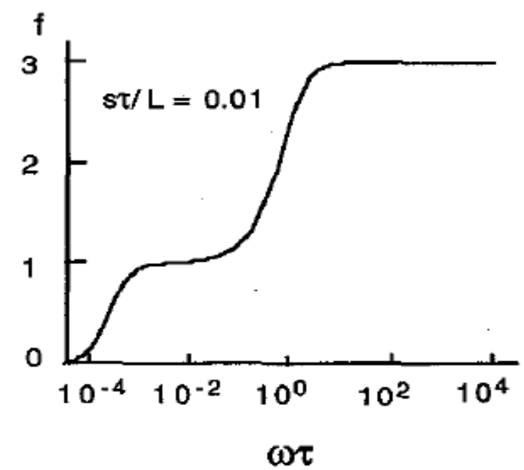

*IEEE TRANSACTIONS ON ELECTRON DEVICES, VOL. 43, NO. 3, MARCH 1996

Experiment: GaAs high-mobility FETs

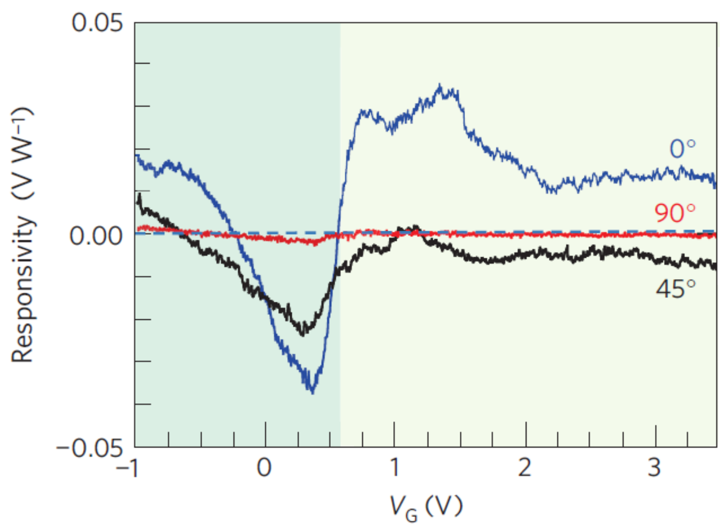

Vicarelli et.al. Nat. Mater. **11**, 865 (2012)
R_{max}=100 mV/W, *f*=300 GHz

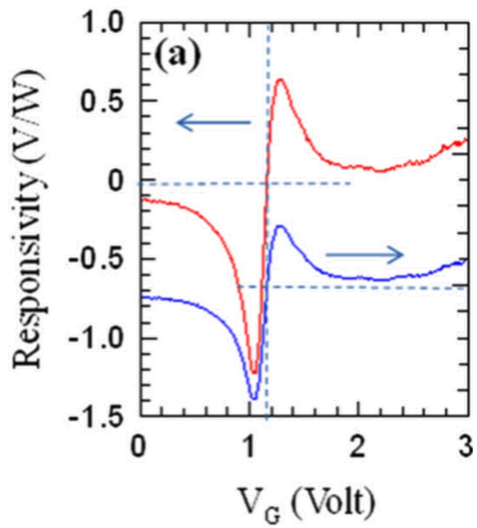

Spirito et.al. APL **104**, 061111 (2014)
R_{max}=1 V/W, *f*=300 GHz

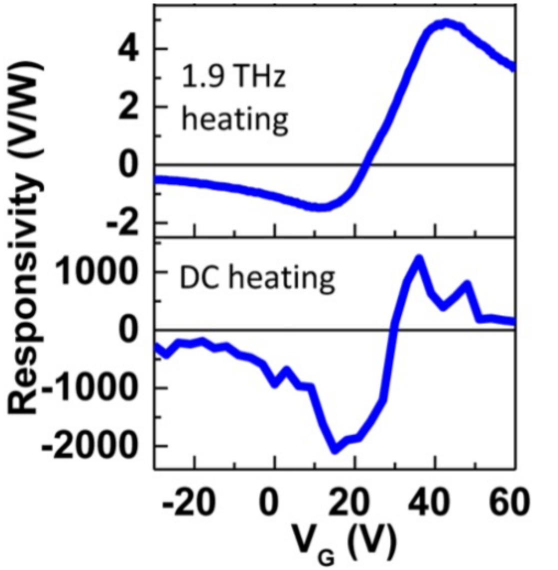

Tong et.al. Nano Lett. **15**, 5295 (2015)
R_{max}=5 V/W, *f*=1.9 THz

Measured responsivities of graphene-based THz detectors vs. gate voltage obtained by various groups to date. In all setups, THz radiation if fed between source and gate, the signal is read out between source and drain

$$Q = 2\pi f_{\mathrm{res}} \tau_p >> 1$$

$$\mu = 10\,000\ \mathrm{cm}^2/(\mathrm{V\,s}) \Rightarrow \tau_p = m^* \mu / e \approx 0.1\ \mathrm{ps}$$

$$Q(1\ \mathrm{THz}) \approx 0.6$$

$$\Delta u = \frac{U_a^2}{4} \frac{1}{\sigma(U_0)} \left. \frac{d\sigma(V_G)}{dV_G} \right|_{V_G = U_0}$$

Resonant terahertz detection using graphene plasmons

There are three crucial steps to consider in the design of resonant photodetectors.

First, the incoming radiation needs to be efficiently compressed into plasmons propagating in the FET channel.

Second, the channel should act as a high-quality plasmonic cavity, where constructive interference of propagating plasma waves leads to the enhancement of the field strength.

Third, the high-frequency plasmon field needs to be rectified into a dc photovoltage.

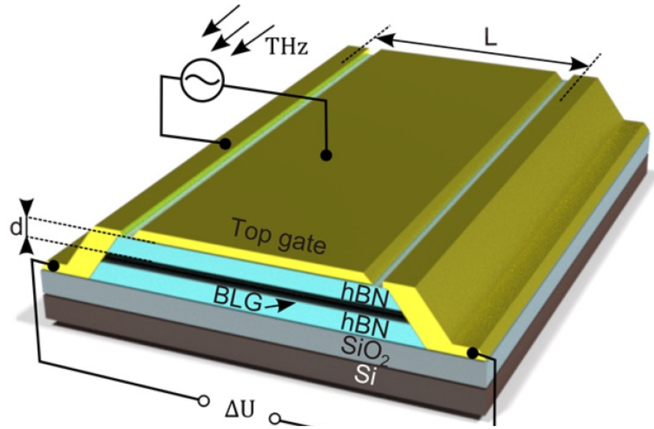

$$s = v_F\sqrt{4\alpha_c k_F d} \approx \sqrt{\frac{e}{m}|V_g|}$$

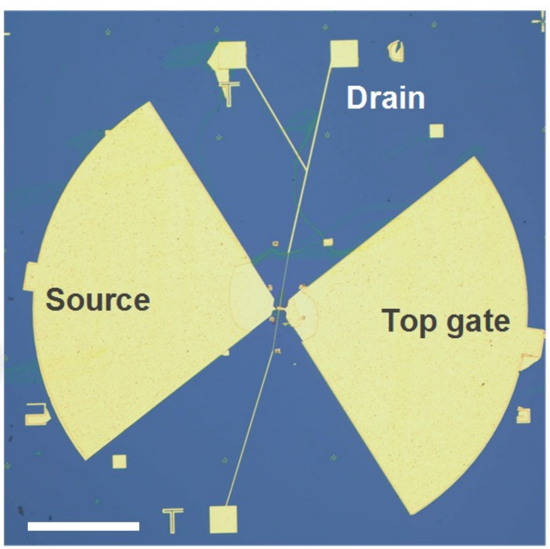

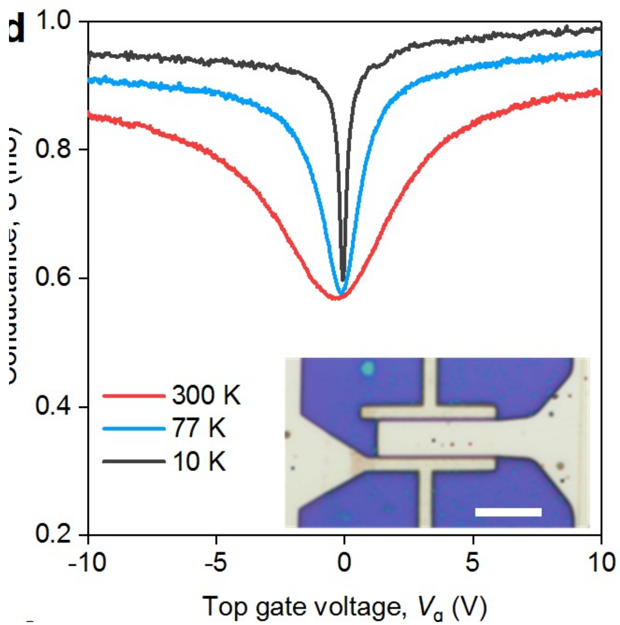

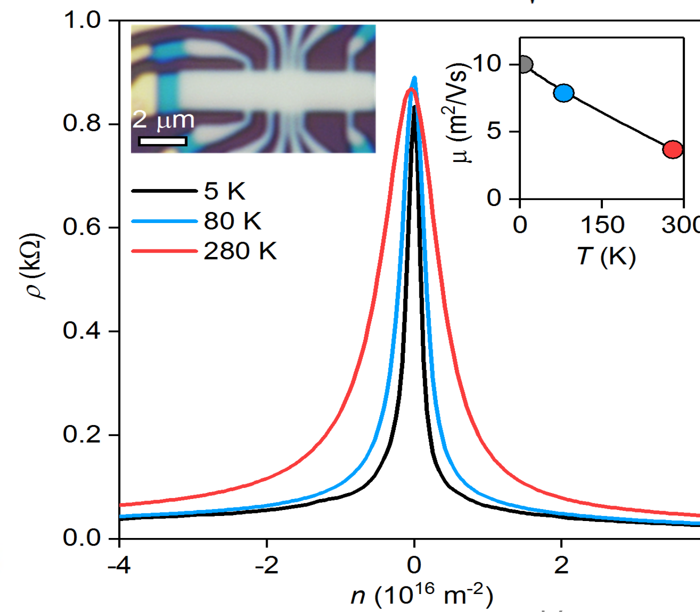

*NATURE COMMUNICATIONS | (2018) 9:5392 | https://doi.org/10.1038/s41467-018-07848-w

Broadband detection

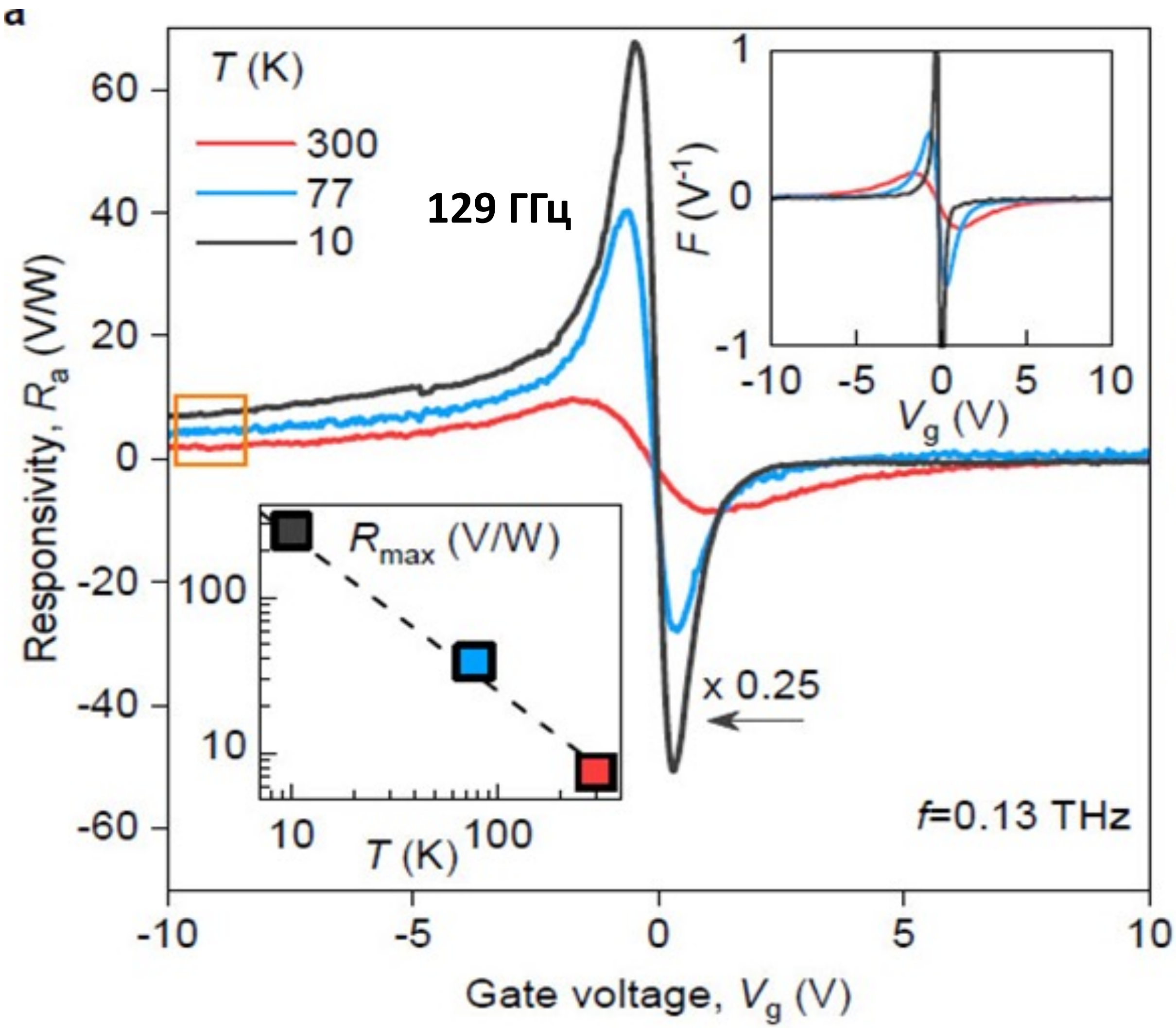

Quality factor 129 GHz

$$Q = 2\pi f \tau_p = 0.2 \ldots 0.7$$

Broadband DS datection

$$\Delta U_{DS} = \frac{U_a^2}{4}\frac{1}{\sigma}\frac{d\sigma}{dV_{bg}} g(\omega) \propto U_a^2 F,$$

$$F = \frac{1}{\sigma}\frac{d\sigma}{dV_{bg}}.$$

Photo-thermoelectric effect

$$U_{PTE} = -\int S dT \approx S(T_S - T_D)$$

$$S \approx -\frac{\pi^2 k_B^2 T}{3e}\frac{1}{\sigma}\frac{d\sigma}{dE_F}$$

*NATURE COMMUNICATIONS | (2018) 9:5392 | https://doi.org/10.1038/s41467-018-07848-w

Broadband detection

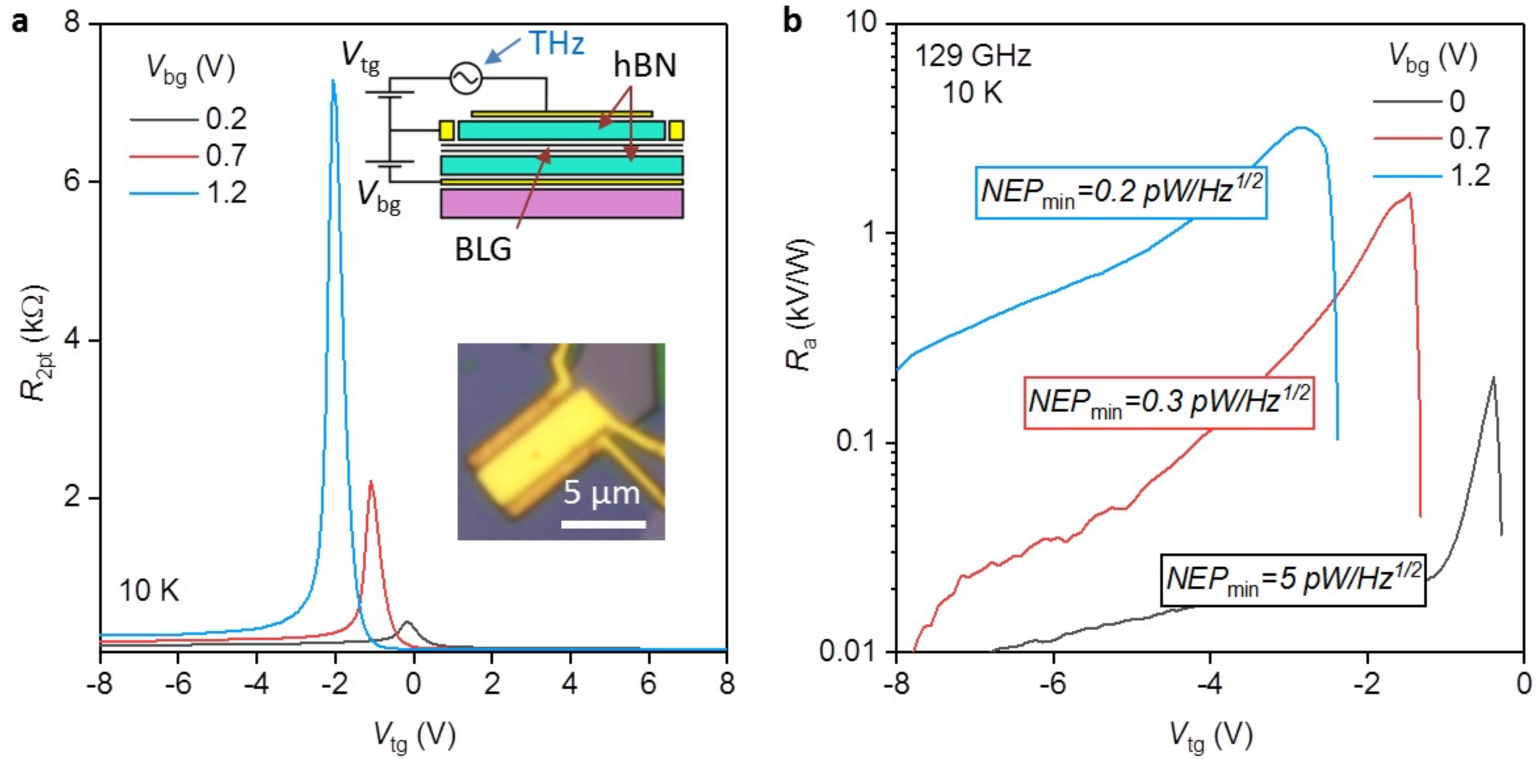

Photoresponse of a dual-gated BLG detector. a, Two-terminal resistance as a function of Vtg measured in a dual-gated BLG FET for different Vbg. Top inset: Schematic of a dual-gated THz detector. Bottom inset: Optical photographs of the device. b, Responsivity as a function of Vtg for different Vbg measured at given f and T.

$$D=\frac{\varepsilon}{2}(V_{tg}/d_{bg} + V_{bg}/d_{tg})$$

*NATURE COMMUNICATIONS | (2018) 9:5392 | https://doi.org/10.1038/s41467-018-07848-w

Resonant detection

129 ГГц → **2 ТГц**

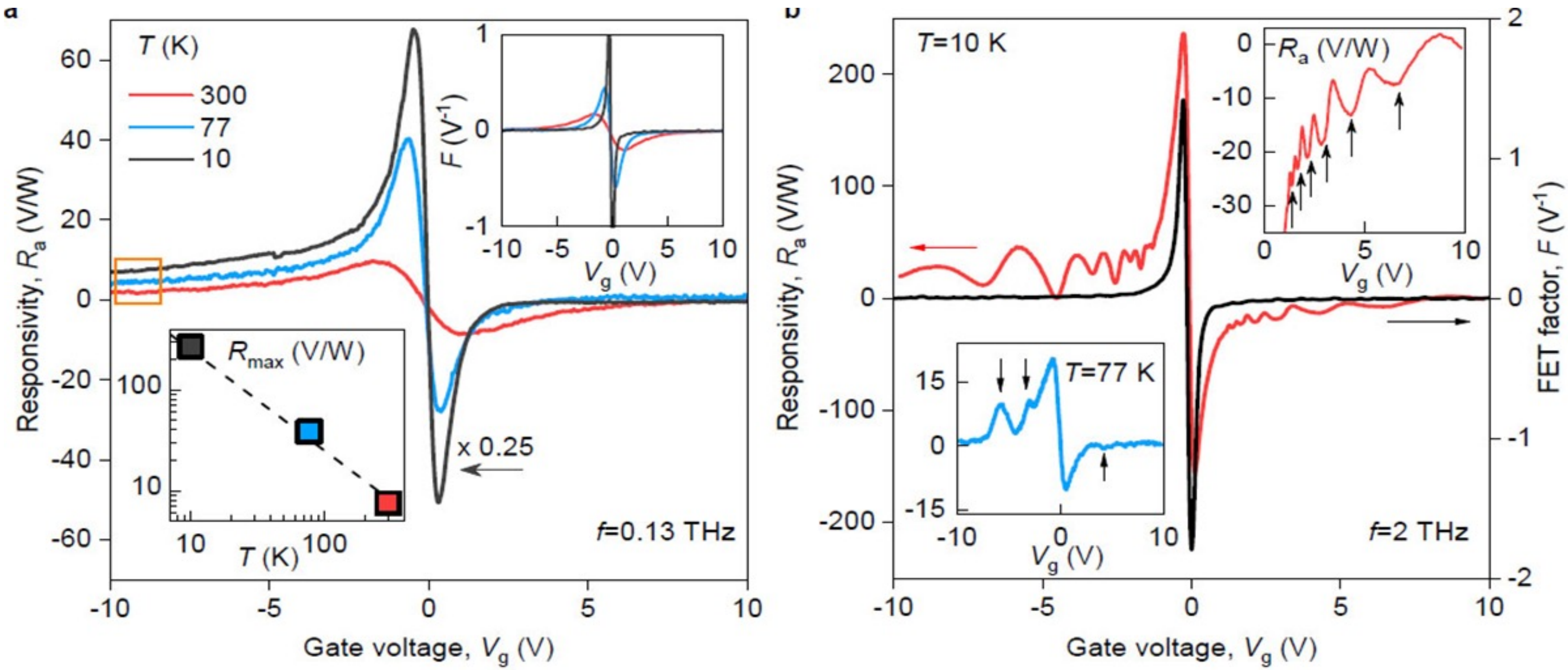

$$s = v_F\sqrt{4\alpha_c k_F d} \approx \sqrt{\frac{e}{m}|V_g|}$$

*NATURE COMMUNICATIONS | (2018) 9:5392 | https://doi.org/10.1038/s41467-018-07848-w

Resonant detection

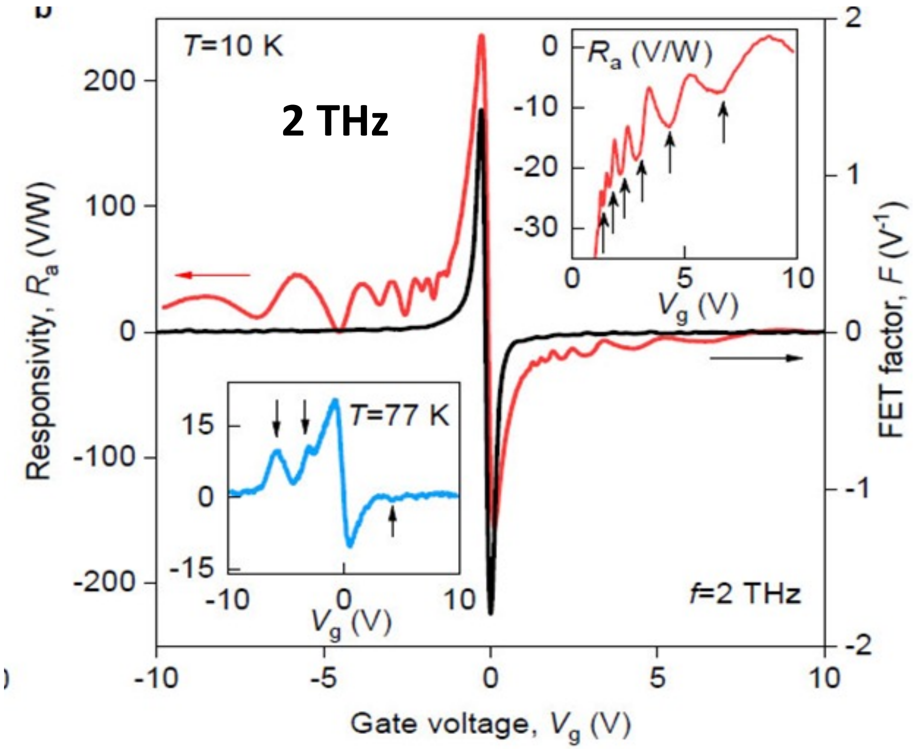

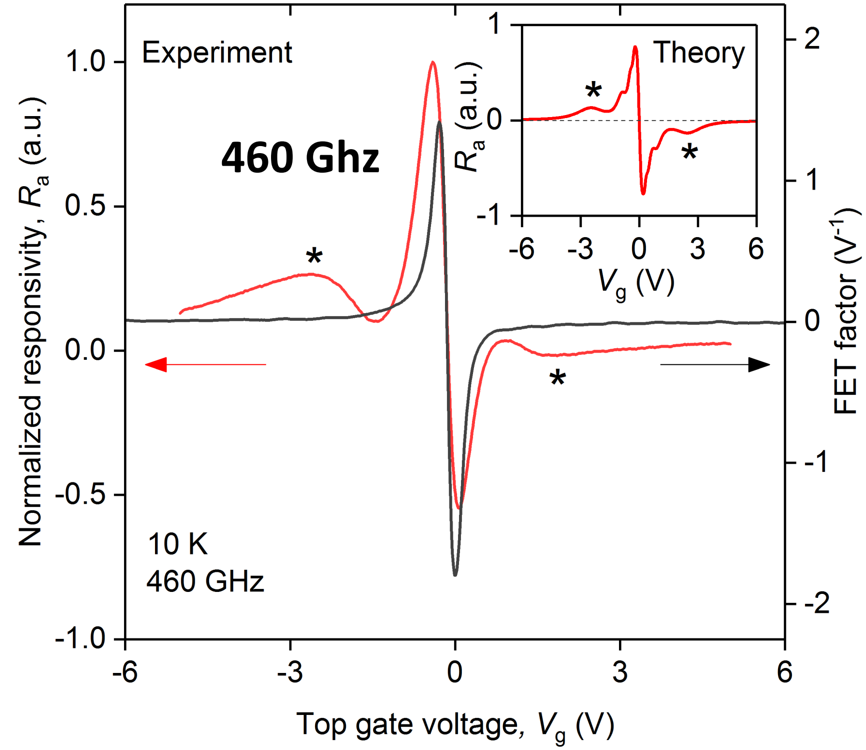

$$s = v_F \sqrt{4\alpha_c k_F d} \approx \sqrt{\frac{e}{m}|V_{\mathrm{g}}|}$$

*NATURE COMMUNICATIONS | (2018) 9:5392 | https://doi.org/10.1038/s41467-018-07848-w

Resonant detection

Theoretical responsivity of our FET as a plasmonic Fabry-Perot cavity endowed with a rectifying element :

$$R_a = \frac{R_0}{|1 - r_s r_d e^{2iqL}|^2}$$

where R_0 is a smooth function of carrier density n and frequency f that depends on the microscopic rectification mechanism, r_s and r_d are the wave reflection coefficients from the source and drain terminals, respectively, and q is the complex wave vector governing the wave propagation in the channel

Resonance conditions: $1 - r_s r_d e^{2iqL} = 0$ In case of $r_s r_d \approx -1$: $q' = \frac{\pi}{2L}(2k+1),$

Plasma wave velocity in 2D system: $s = v_F\sqrt{4\alpha_c k_F d} \approx \sqrt{\frac{e}{m^*}|V_g|}$

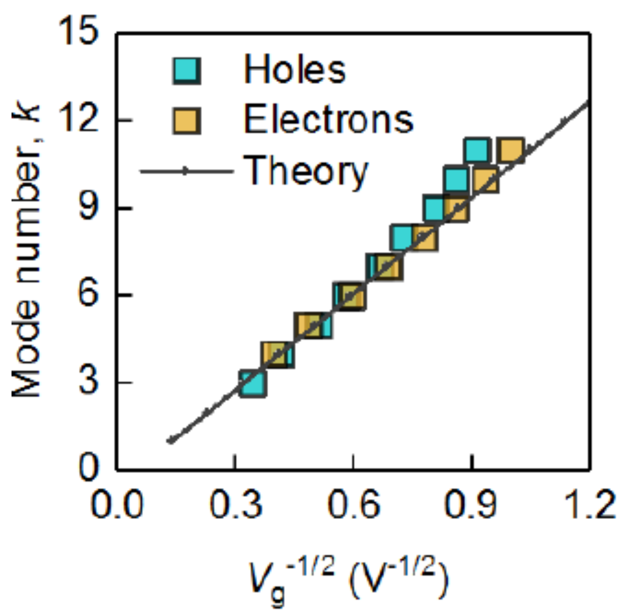

*NATURE COMMUNICATIONS | (2018) 9:5392 | https://doi.org/10.1038/s41467-018-07848-w

THz plasmon spectroscopy at 10 K

The resonant gate-tunable response of our detectors offers a convenient tool to characterize plasmon modes in graphene channels

Plasma wave velocity in 2D system: $s = v_F\sqrt{4\alpha_c k_F d} \approx \sqrt{\frac{e}{m^*}|V_g|}$

$$q' = \frac{\pi}{2L}(2k+1),$$

L=(2k+1)λp/4, where λp =2π/q'

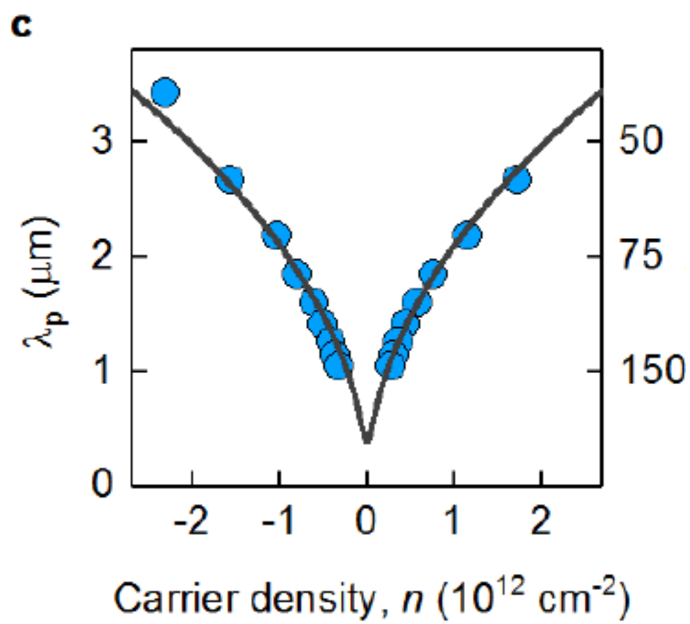

*NATURE COMMUNICATIONS | (2018) 9:5392 | https://doi.org/10.1038/s41467-018-07848-w

THz plasmon spectroscopy at 10 K

Theoretical responsivity of our FET as a plasmonic Fabry-Perot cavity endowed with a rectifying element :

$$R_a = \frac{R_0}{|1 - r_s r_d e^{2iqL}|^2}$$

where R_0 is a smooth function of carrier density n and frequency f that depends on the microscopic rectification mechanism, r_s and r_d are the wave reflection coefficients from the source and drain terminals, respectively, and q is the complex wave vector governing the wave propagation in the channel

Plasmon lifetime:

$$\frac{\delta V_g^{-1/2}}{V_g^{-1/2}} = \frac{1}{\omega \tau_p}$$

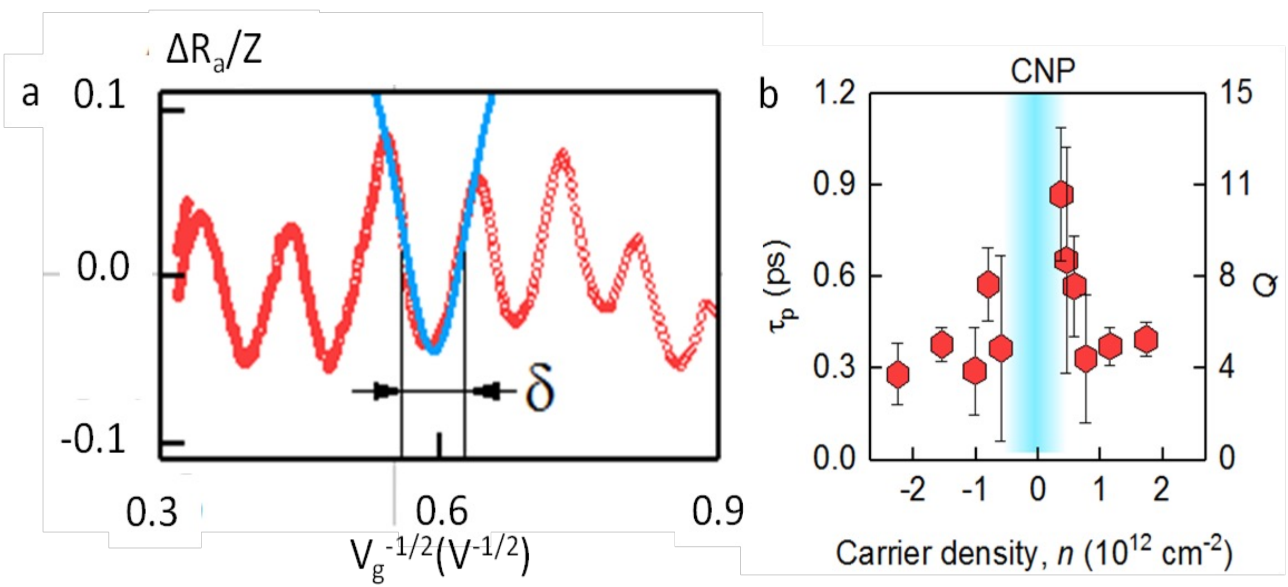

*NATURE COMMUNICATIONS | (2018) 9:5392 | https://doi.org/10.1038/s41467-018-07848-w

Conclusion

1. We have shown that high-mobility graphene FETs exploiting far-field coupling to incoming radiation can operate as resonant THz photodetectors.
2. Our devices represent a convenient tool to study plasmons under conditions where other approaches may be technically challenging. Due to their compact size and far-field coupling, our photodetectors can easily be employed to carry out plasmonic experiments in extreme cryogenic environments and in strong magnetic fields, as well in studies of more complex van der Waals heterostructures.

***NATURE COMMUNICATIONS | (2018) 9:5392 | https://doi.org/10.1038/s41467-018-07848-w**

Collaboration

. Gayduchenko, M. Moskotin, N. Titova, B. M. Voronov, N. Kaurova, G. N. Goltsman, **MPSU, Moscow, Russia**

G. Fedorov ,D. Svintsov, ***MIPT, Russia***

D. Bandurin, ***The University of Manchester, UK***

Thank you for attention!!!

Полевые транзистора в конфигурации Дьяконова Шура с графеновым каналом для детектирования ТГц излучения

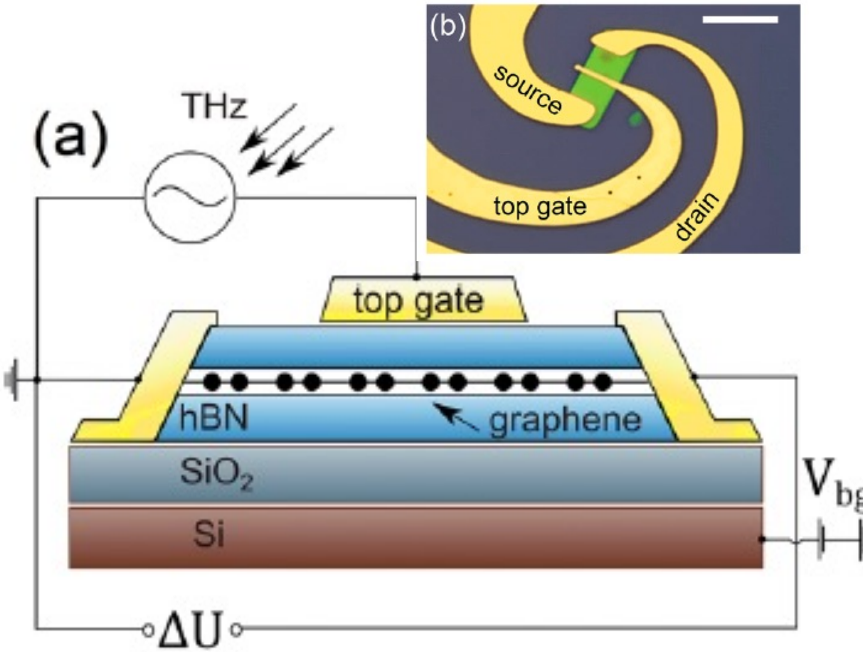

Схема полевого транзистора с графеновым каналом

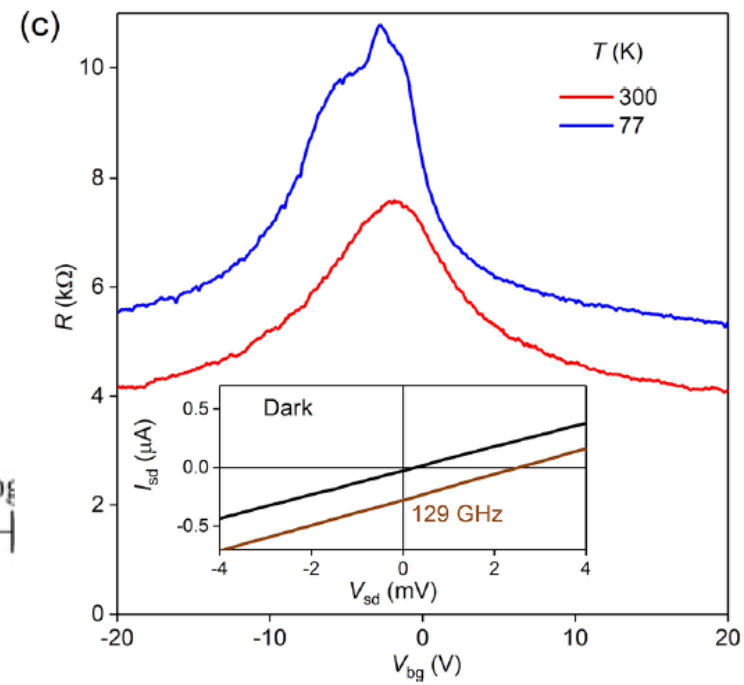

Зависимость двухконтактного сопротивления затворного напряженя

RT mobility

$$\mu = 3200\ cm^2 V^{-1} s^{-1}$$

D. A. Bandurin, I. Gayduchenko, et al., Applied Physics Letters112, 141101, (2018)

Полевые транзистора в конфигурации Дьяконова Шура с графеновым каналом для детектирования ТГц излучения

Отклик полевых транзисторов на излучение 129 ГГц при температутре 300К и 77К

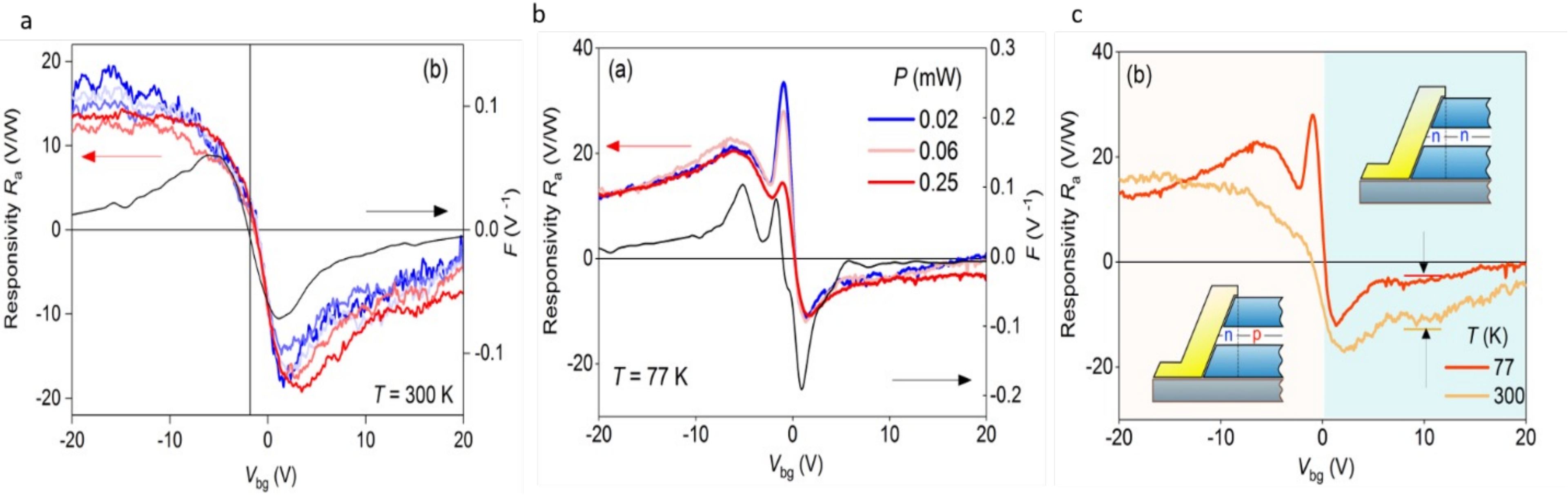

Фото-термоэлектрический эффект

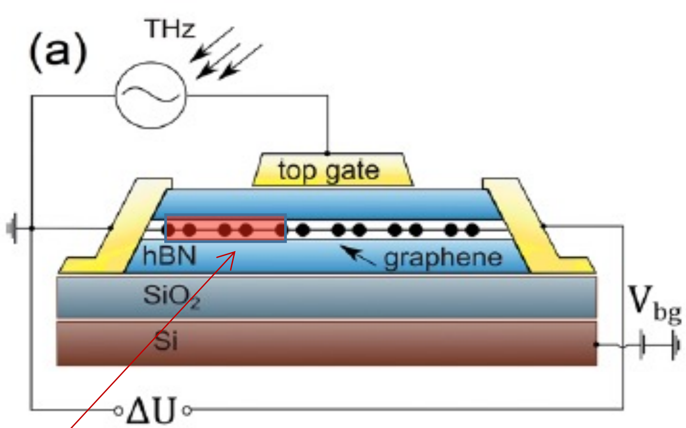

$$U_{PTE} = -\int S dT \approx S(T_S - T_D)$$

$$S \approx -\frac{\pi^2 k_B^2 T}{3e}\frac{1}{\sigma}\frac{d\sigma}{dE_F}$$ is the Seebeck coefficient

$$F = \frac{1}{\sigma}\frac{d\sigma}{dV_{bg}}.$$

Перегретая область

D. A. Bandurin, I. Gayduchenko, et al., Applied Physics Letters112, 141101, (2018)

Фото-термоэлектрический эффект

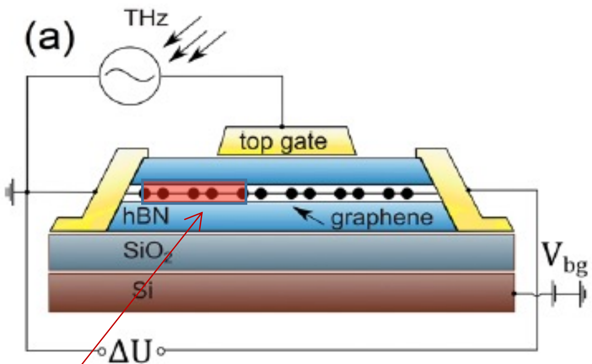

Перегретая область

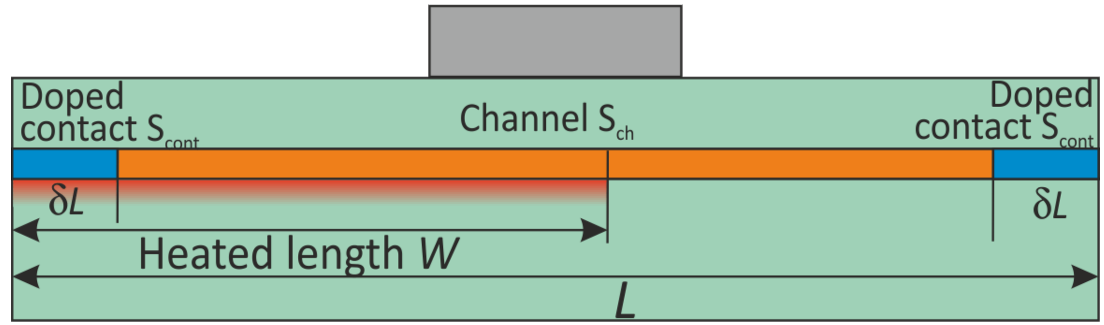

$$U_{PTE}=(S_{ch}\text{-}Sc_{ont})(T_S\text{-}T_D)$$

$$R_a \approx \frac{3}{2\pi^2}\left[\frac{e}{k_B}(S_{\text{cont}}-S_{\text{ch}})\right]\frac{eZ_a}{k_B T}\frac{\delta L}{L},$$

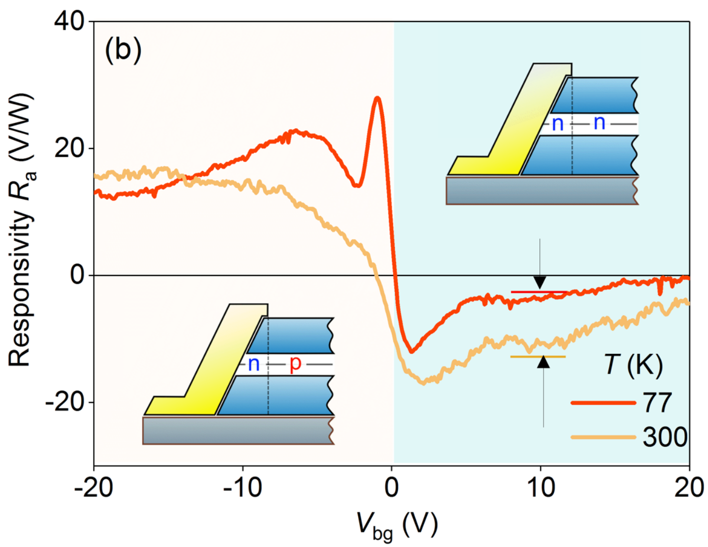

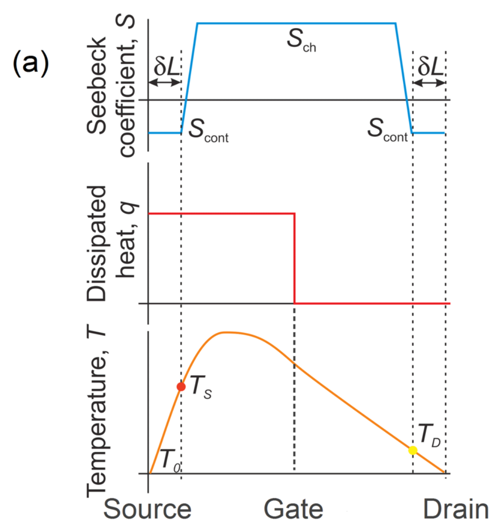

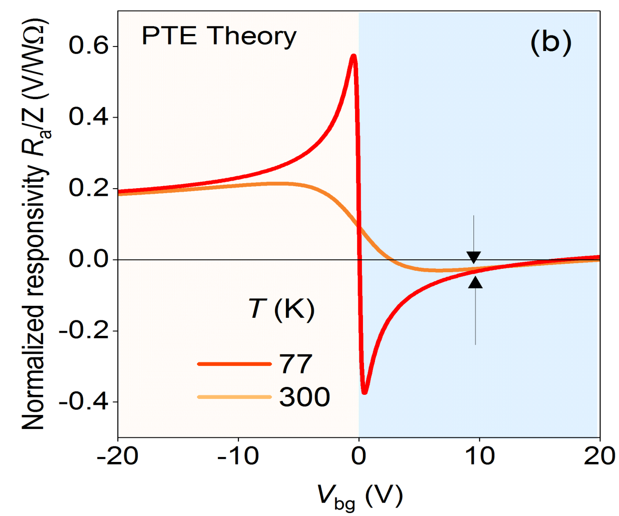

D. A. Bandurin, I. Gayduchenko, et al., Applied Physics Letters112, 141101, (2018)

Эффект Дьконова-Шура

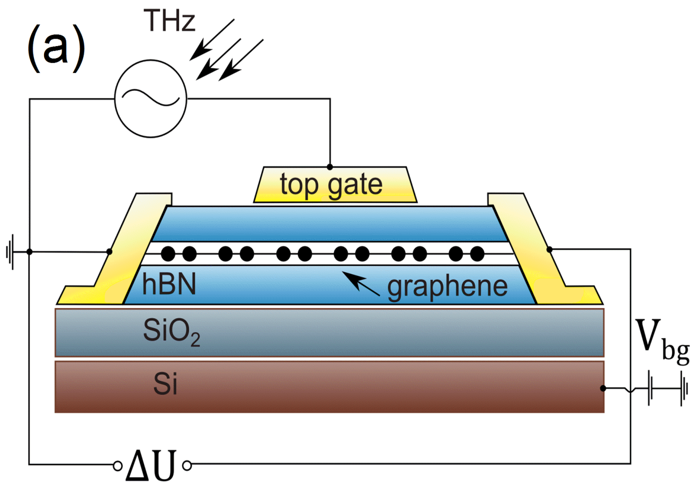

$$\Delta U_{\mathrm{DS}} = \frac{U_{\mathrm{a}}{}^2}{4}\frac{1}{\sigma}\frac{d\sigma}{dV_{\mathrm{bg}}} g(\omega) \propto U_{\mathrm{a}}{}^2 F$$

Где U_{a} – напряжение на антенне, L – длина канала, $g(\omega) = (\sinh^2 kL - \sin^2 kL)/(\sinh^2 kL + \cos^2 kL)$ - форм фактор, зависящий от волнового числа $k = \sqrt{\omega/(2s^2\tau)}$ затухающей плазменной волны, характеризающейся групповой скоростью $s = \sqrt{4\alpha_{ee} d\sqrt{\pi n}}$

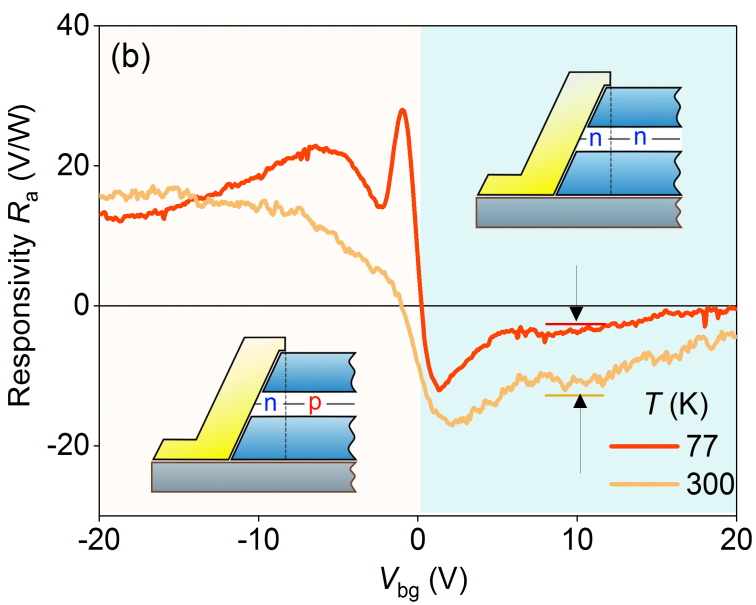

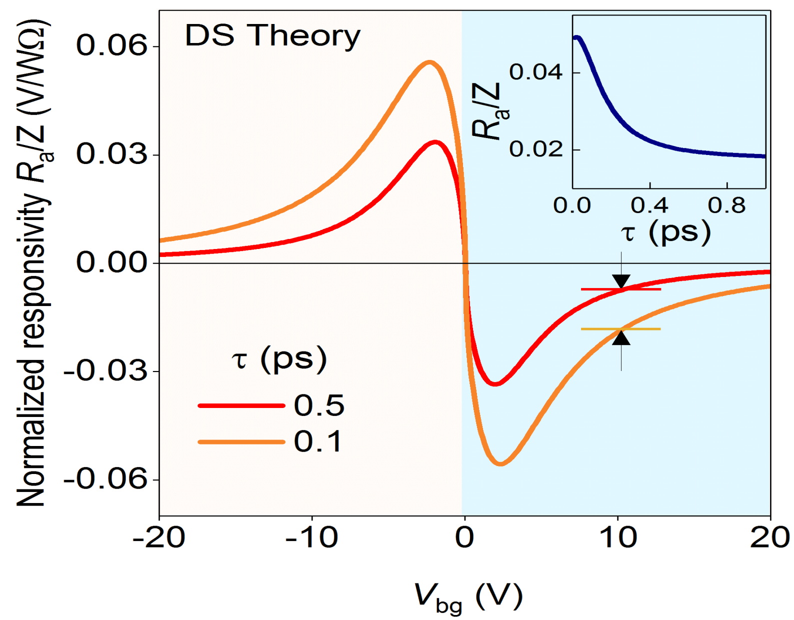

D. A. Bandurin, I. Gayduchenko, et al., Applied Physics Letters112, 141101, (2018)